ELSEVIER

Journal of Organometallic Chemistry 640 (2001) 170–176

Journal of Organometallic Chemistry

www.elsevier.com/locate/jorganchem

UV laser-induced photolysis of 1,3-disilacyclobutane in oxygen for chemical vapour deposition of nano-sized polyoxocarbosilane films

Josef Pola [a,*], Josef Vítek [a], Zdeněk Bastl [b], Jan Šubrt [c]

[a] *Laser Chemistry Group, Institute of Chemical Process Fundamentals, Academy of Sciences of the Czech Republic, Rozvojova Str. 135, 165 02 Prague 6, Czech Republic*
[b] *J. Heyrovský Institute of Physical Chemistry, Academy of Sciences of the Czech Republic, 182 23 Prague 8, Czech Republic*
[c] *Institute of Inorganic Chemistry, Academy of Sciences of the Czech Republic, 25 068 Řež near Prague, Czech Republic*

Received 11 June 2001; accepted 10 August 2001

Dedicated to Professor M.G. Voronkov in recognition of his important contributions to organosilicon chemistry

---

Abstract

The multi-pulse ArF laser irradiation into gaseous 1,3-disilacyclobutane–O_2 mixture in excess of buffer gas occurs as non-explosive chemical vapour deposition of solid methylsilicone films, whereas the single-pulse irradiation into the gaseous mixture in the absence of buffer gas results in explosive chemical vapour deposition of solid nano-structured polyoxocarbosilanes poor in hydrogen. © 2001 Elsevier Science B.V. All rights reserved.

Keywords: 1,3-Disilacyclobutane; Silene; Oxidation; Laser photolysis; Nanostructured polyoxocarbosilane

---

1. Introduction

There is continuing interest in Si:C:O:H and Si:O:H phases due to their importance in applied materials research [1,2]. They can be produced by pyrolysis of polysiloxanes [3] or polysiloxane gels [4], by pyrolytic laser–aerosol interaction [5] and by plasma- [6] or laser- [7] interaction with gaseous organosilanes, whereas the Si:O:H phases can be formed in plasma of silane and oxygen [2], by oxidation of Si:H films [8] and by UV laser- [9] or IR laser- [10] induced decomposition of disiloxane.

Another route to these materials may be gas-phase decomposition of silacyclobutanes or 1,3-disilacyclobutanes (DSCB) (I)

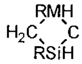

(I)

(M = C, Si; R = alkyl, H) conducted in the presence of molecular oxygen. These silacycles are known [11] to split to silenes $RHSi{=}CH_2$ in equilibrium with the isomeric silylenes: $Si(R)CH_3$.

The photolytical or thermal reaction of both species with $^3O_2$ at low-temperatures of cryogenic matrices [12–16] yields reactive oxygen-containing organosilicon compounds like dioxasiliranes, silaesters, siladioxetanes and silanones. The oxidation of silenes generated in the gas phase by conventional low-pressure thermolysis of 1,1-dimethyl-1-silacyclobutane yields cyclic poly(dimethylsiloxanes) $(Me_2SiO)_n$ ($n = 3$, 4) and oxacarbosilanes $[(Me_2SiO)_n(Me_2SiCH_2)_m$ (n, $m = 1$, 2) along with formaldehyde and ethene and was interpreted [17] as in Scheme 1.

We have reported that IR laser-induced thermolysis and UV laser-induced photolysis of various silacyclobutanes and DSCB in the gas phase yields transient silenes

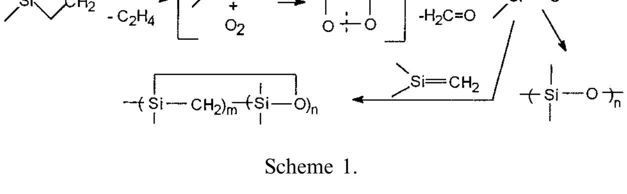

Scheme 1.

---

* Corresponding author. Tel.: +420-2-203-90308; fax: +420-2-209-20661.

E-mail address: pola@icpf.cas.cz (J. Pola).

0022-328X/01/$ - see front matter © 2001 Elsevier Science B.V. All rights reserved.

PII: S0022-328X(01)01183-4

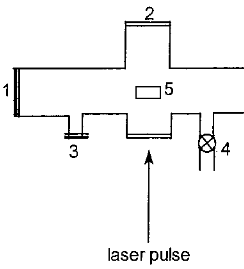

Fig. 1. Pyrex reactor. 1, KBr window; 2, quartz window; 3, rubber septum; 4, PTFE valve; 5, substrate.

(and silylenes) that, perhaps due to being generated in high concentrations, do not cyclodimerize, but efficiently gas-phase polymerize into solid saturated polycarbosilane films [18–22].

It was of further interest to examine one of these reactions in the presence of oxygen and determine in which way oxygen intervenes with formation of polycarbosilanes. Here we present the examination of ArF laser-induced photolysis of DSCB [18] in the presence of molecular oxygen and show that this reaction affords solid polyoxocarbosilane deposit with H content affected by the presence of buffer gas.

2. Experimental

Laser photolysis experiments were carried out on gaseous mixture of DSCB and O_2 (both 0.7 kPa) in the absence or at atmospheric pressure of helium or nitrogen using an ArF (ELI 94 model) laser operating at 193 nm with a repetition frequency of 1 Hz. The samples were irradiated in a Pyrex reactor consisting of two orthogonally positioned tubes (both 3 cm in diameter), one (13 cm in length) furnished with KBr windows and the other (9 cm in length) equipped with quartz windows. The reactor had two side arms, one fitted with a rubber septum and the other connecting to a standard vacuum manifold (Fig. 1). The reactor accommodated metal and KBr substrates, which, covered with the solid material deposited in the course of irradiation, were transferred for measurements of their properties by photoelectron and FTIR spectroscopy as well as electron microscopy. The metal substrates were washed by acetone in an ultrasonic bath. The laser beam at fluence of 60 mJ effective on area of 1.7 cm^2 was used.

The progress of photolysis was monitored directly in the reactor by infrared spectroscopy (an FTIR spectrometer Nicolet Impact 400) and also, after admitting helium into the reactor to atmospheric pressure, by gas chromatography (a Shimadzu 14A chromatograph with Porapak P or SE-30 columns, programmed (20–150 °C) temperature, He carrier gas). The gaseous products were identified by FTIR and GC–MS spectrometry (a QP 1000 Shimadzu spectrometer, Porapak P column, programmed (20–150 °C) temperature, He carrier gas) and also by comparison of their GC retention times with those of authentic samples.

The depletion of DSCB was followed using a diagnostic band at 779 cm^{-1} and formation of ethyne and methane was observed at 730 and 1305 cm^{-1}, and that of formaldehyde, MeOH and formic acid at 1745, 1034 and 1775 cm^{-1}, respectively.

Quantitative GC analyses were performed using the FID response factors as follows: hydrocarbons (1.0), formaldehyde and formic acid (0.01) and methanol (0.23). The sampling was conducted using a gastight syringe.

The FTIR spectra of the deposits on KBr windows, as well as on KBr substrates were recorded after evacuation of the reactor.

The X-ray photoelectron spectra were acquired using a VG ESCA 3 Mk II electron spectrometer employing Al–K$_\alpha$ radiation. X-ray excited Auger electron spectra were obtained using bremsstrahlung radiation. High resolution spectral scans were taken over Si 2p, Si KL$_{23}$ L$_{23}$, C 1s and O 1s regions. Pressure of residual gases during spectra measurement did not exceed 10^{-6} Pa. Quantification of the element surface concentration ratio was accomplished by correcting integral intensities of photoelectron spectra for pertinent cross-sections [23] and accounting for the dependence of electron analyzer transmission on the kinetic energy of electrons [24].

Scanning electron microscopy of the deposits was carried out with a Tesla BS 350 microscope and transmission electron microscopy measurements were performed on a Philips 201 microscope. Materials deposited on Al substrates were analyzed by SEM technique and when scrubbed from the substrate and held with a copper grid by TEM analysis.

DSCB was synthesized according to earlier reported procedure [25] and its purity was better than 99%. Compounds used as the standards for the analysis of the FTIR spectra of the irradiated DSCB–O_2–He mixture were from the laboratory stock (CO, CH_3OH) or freshly prepared [26] by standard techniques (H_2CO, HCOOH). Their purity was checked by FTIR spectroscopy and gas chromatography.

3. Results and discussion

Gaseous DSCB exerts UV absorption above 190 nm [18] with absorptivity 18×10^{-2} kPa^{-1} cm^{-1} at the irradiating wavelength of ArF laser (193 nm). The energy delivered by the 193 nm photons corresponds to ca. 620 kJ mol^{-1} and is in excess of the activation energy for cleavage of the four-membered ring of DSCB (230 kJ mol^{-1}, Ref. [27]) to yield silene. The laser irradiation of gaseous DSCB–O_2 mixture in the

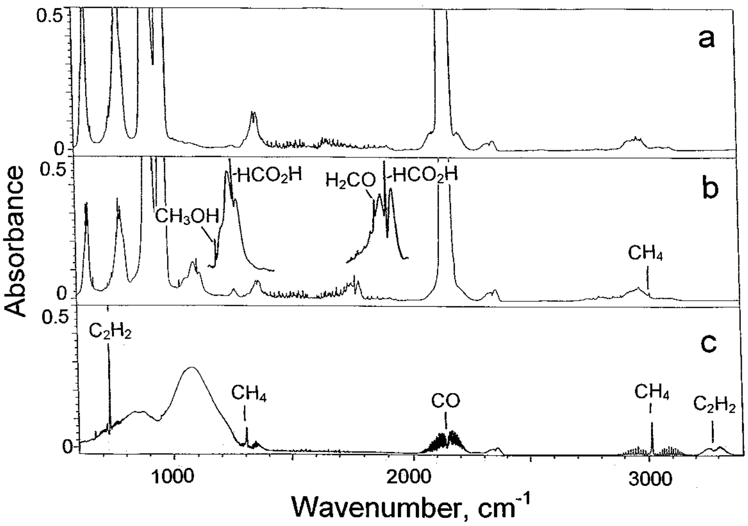

Fig. 2. Typical FTIR spectrum of the initial DSCB–O_2 mixture (a), DSCB–O_2–He mixture after 300 pulses (b) and DSCB–O_2 mixture after single pulse (c) photolysis.

absence of inert gas (N_2 or He) takes place as an explosive reaction which is accomplished within a single laser pulse, whereas the irradiation of the DSCB–O_2 mixture in excess of helium or nitrogen is a much slower process in which about 50% of DSCB depletes with as many as 300 pulses. A discussion for each mixture is given below.

3.1. Multi-pulse non-explosive photolysis

The irradiation of the DSCB–O_2 (each 0.7 kPa) in excess of inert gas (He or N_2, total pressure 53 kPa) does not show any visible luminescence. It yields (in relative molar per cent) formaldehyde (65–80), methanol (5–10), formic acid (8–10), ethene (2–5) and methane (2–3) as the volatile products detectable by FTIR (Fig. 2) and GC–MS spectra and quantified by GC analysis (Fig. 3). It also results in the deposition of a whitish solid film. Typically, ca. 50% of DSCB was depleted in as many as 300 pulses.

3.2. Single-pulse explosive photolysis

The irradiation of the DSCB–O_2 (each 0.7 kPa) with the single pulse results in an explosive reaction. A whitish luminescence is observed and DSCB is completely depleted. Typical IR spectral changes are given in Fig. 2. Ethyne, methane and carbon monoxide were detected by FTIR spectra. GC and GC–MS analysis revealed that the hydrocarbons are produced in ratios C_2H_2:CH_4:C_2H_4 = 1:0.5:0.03 (Fig. 3). Concomitantly, the whitish solid film was deposited onto the reactor surface.

3.3. Properties of deposited materials

X-ray photoelectron spectroscopy study of the solid deposits from the explosive and non-explosive photolysis confirms that both are composed of silicon, carbon and oxygen and that their stoichiometry is $Si_{1.00}C_{1.06}O_{1.11}$ and $Si_{1.00}C_{0.90}O_{1.33}$, respectively. The observed values of Si 2 p core-level binding energies (both 102.6 ± 0.2 eV, Fig. 4), the calculated value of the Auger parameters (both 1711.7 ± 0.2 eV, Fig. 5), and also the values of C 1s core level binding energies (both 284.7 ± 0.2 eV) are consistent with data reported in the literature for polymethylsilicone [28] and methyl(hy-

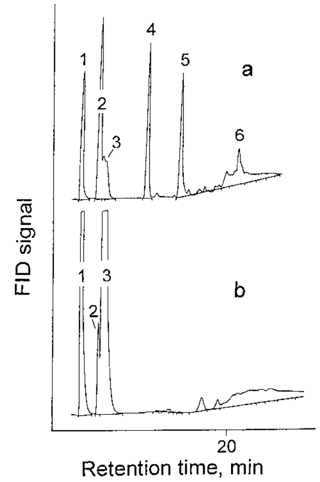

Fig. 3. Typical GC trace of DSCB–O_2–He mixture after 300 pulses (a) and DSCB–O_2 mixture after single pulse (b) photolysis. Porapak P column, peak designation: 1, CH_4; 2, C_2H_4; 3, C_2H_2; 4, H_2CO; 5, CH_3OH; 6, HCO_2H.

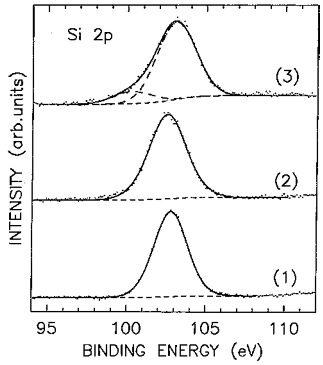

Fig. 4. Photoelectron spectra of Si(2p) electrons. Deposit from single-pulse explosive photolysis (1) and multi-pulse non-explosive photolysis before (2) and after (3) Ar^+ ion sputtering.

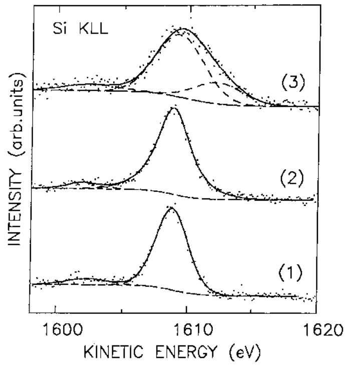

Fig. 5. Spectra of Si ($KL_{23}L_{23}$) Auger electrons. Designation as in Fig. 4.

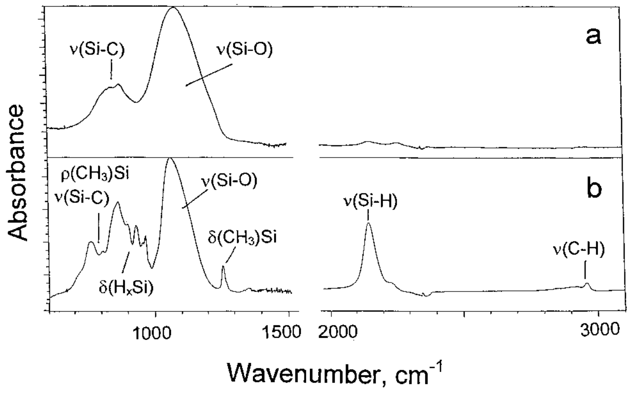

Fig. 6. Typical FTIR spectrum of the solid deposit from the single-pulse (a) and multi-pulse (b) photolysis.

drido)silicone [7] phases. Occurrence of the additional, weak component in the spectra of the sample sputtered by argon ions is most likely due to the inhomogeneity of the static charging of this sample. This explanation is corroborated by the fact that both components give the same value of the Auger parameter thus showing that identical chemical states of Si are involved.

FTIR spectra of the solids from the non-explosive and explosive photolysis differ (Fig. 6). The former consists of bands at ν [cm^{-1}] (relative absorbance) 760 (0.36), 862 (0.64), 930 (0.50), 963 (0.40), 1058 (1.0), 1258 (0.16), 2148 (0.50), 2233 (0.04) and 2924 (0.04) which are assignable, in the given order, to ν(Si–C), δ(SiH$_x$), ν(Si–O) (possibly contributed by ν(SiCH$_2$Si), ν(C–O), δ(CH$_3$Si), ν(Si–H) and ν(C–H) vibrations. The latter shows a broad (major) band at 1087 cm^{-1} along with weaker bands at 875 and 844 cm^{-1} of relative absorbance 0.34. This pattern is in keeping with the presence of Si–O and Si–C bonds and the absence of Si–H and C–H bonds.

It is known that the oxygen and H$_n$Si bending modes below 1000 cm^{-1} in amorphous SiO$_x$:H films ($x < 2$) and oxygenated polysilanes [29–32] are less informative [33], while the Si–H stretching mode in polysilanes is empirically related to the electronegativity/inductive effect of the neighbouring atoms [34,35]. It is also known that fully oxidized (SiH$_2$)$_x$ polysilanes exhibit [36] bands at 2190 and 2245 cm^{-1}. The bands at 2148 and 2233 cm^{-1} observed in the deposited solid from the non-explosive photolysis (Fig. 2b) can thus be assigned to the H$_2$Si(O) structural unit. The estimation of the relative content of the Si–O and Si–H bonds by comparing the A_{Si-H}:$A_{Si-O-Si}$ ratio in the deposit (0.5) and in cyclotetrasiloxane (H$_2$SiO)$_4$ (ca. 0.5 [37]) is in line with an important contribution of the (H$_2$SiO)$_n$ formulae and supports this view. The lack of bands at ca. 2100 and 2000 cm^{-1} indicates [36,38] the absence of (SiH$_2$)$_n$ and (SiH)$_n$ structures in which the Si–H bond is isolated from oxygen by at least two silicon atoms.

The films deposited from the non-explosive photolysis are more adhesive to glass, KBr and metal (Cu, Al) and show different morphology than those produced in the explosive photolysis (Fig. 7). TEM analysis reveals that the solids produced during the explosive reaction are composed of nano-structured agglomerates with units size of 10 nm and of nanorods having 10–20 nm diameter and ca. 200 nm length.

The materials from the explosive photolysis are not soluble in common organic solvents (methanol, diethyl ether, toluene, chloroform), whereas those from the non-explosive photolysis are slightly soluble in toluene. These features indicate that the materials have high molecular weight and/or a cross-linked structure.

3.4. Hypothetical photolytic steps

3.4.1. Multi pulse non-explosive photolysis

The observation of formaldehyde is in accord with the reaction scheme in which silene produced by DSCB photolysis [10] undergoes addition of O$_2$($^3\Sigma$) and yields unstable siladioxetane which decomposes into formaldehyde and silanone [17]. The formation of formic acid and methanol indicates partial oxidation of H$_2$CO, as well as its reaction with hydrogen arising from UV photolytic dehydrogenation [9] of H$_2$SiO species and/or

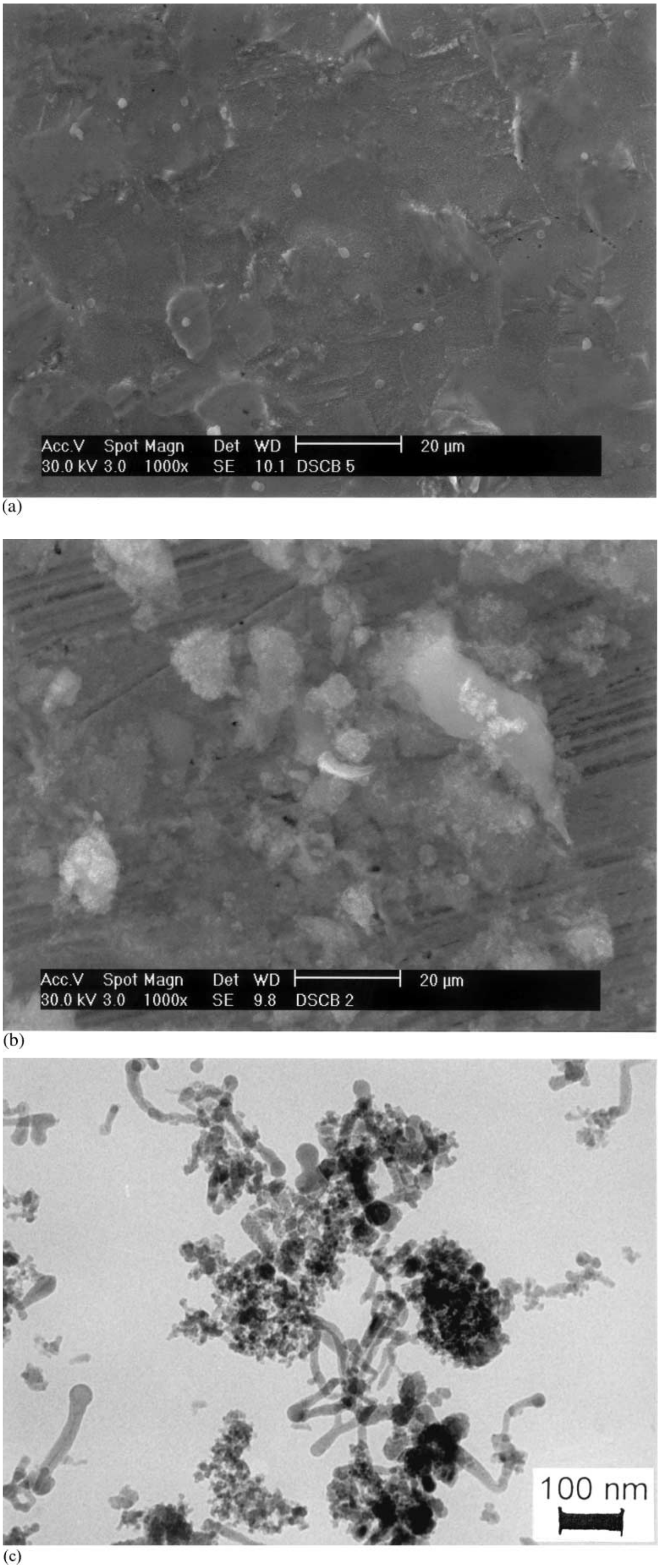

Fig. 7. SEM of solid deposit from non-explosive photolysis (a) and SEM (b) and TEM (c) of solid deposit from explosive photolysis. Al substrate, film thickness ∼1 µm.

of oligomeric $(H_2SiO)_n$. The gaseous silanone $H_2Si{=}O$ is theoretically predicted to undergo no energy barrier polymerization [39] and isomerization [40–42] to hydroxysilylene H(HO)Si: which it may react with to produce hydridosilicone films [10].

However, the observed composition of the solid films shows the important incorporation of carbon. This can primarily originate from reaction of silene with silanone and from insertion of silene [11] into $(H_2SiO)_n$ products, but also from reactions [11] of intermediary silene $H_2Si{=}CH_2$ with the minor nucleophilic products (CH_3OH, H_2CO and HCO_2H). The plausibility of the cycloaddition of silene with H_2CO is supported by the occurrence of ethene, the product not observed in the ArF laser photolysis of DSCB in the absence of oxygen [18]. Other highly probable reactions leading to the final solid methylsilicone product are insertion and addition reactions of methylsilylene [43,44] (the isomer of silene) to silanone and $(H_2SiO)_n$ oligomers. Finally, oxidation [16] of methylsilylene via dioxasilirane to carbonyl compounds ($CH_3Si(O)OH$ or $HSi(O)OCH_3$) can also play a role. These reactions, except the last one, are shown in Scheme 2.

3.4.2. Single pulse explosive photolysis

The observation of CH_4, C_2H_2 (a typical high temperature product) and CO together with the polycarbosilane deposit poor in H is in keeping with the view that the paths assumed for the multi-pulse photolysis are accompanied with high energy demanding homolytic routes. The homolyses possibly include formation of methane via cleavage of intermediary species with CH_3–Si bond, dehydrogenation of formaldehyde into carbon monoxide and dehydrogenation of methylsilicone products. It is known that some steps occurring in the oxidation of silenes and silylenes are highly exothermic [15,16]. Their occurrence together with the absence of cooling effect of buffer gas make the homolytic contributions highly possible. We note similar explosive character of gas-phase laser-driven oxidation of tetrafluoroethene [45].

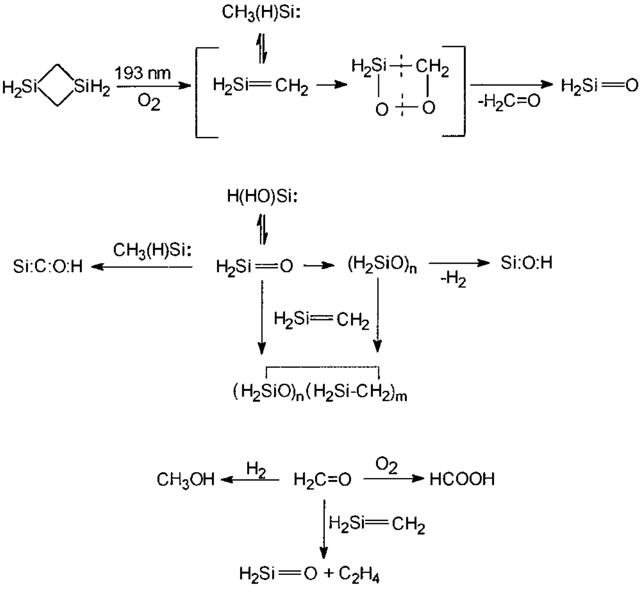

Scheme 2.

4. Conclusion

The ArF laser photolysis of DSCB–O_2 mixtures in the presence buffer gas (N_2, He) is a complex reaction yielding formaldehyde, methanol, formic acid and methane together with solid methylsilicone deposit. It is judged to involve oxidation of silene and cleavage of intermediary dioxetane and can be used for chemical vapour deposition of methylsilicone films.

The ArF laser photolysis of DSCB–O_2 mixtures in the absence of the buffer gas occurs as a single-pulse explosive reaction that yields methane, ethyne, ethene and carbon monoxide along with unique solid nanostructures of Si:C:O phase which can find use in applied science.

Acknowledgements

The research was supported by the Ministry of Education, Youth and Sports of the Czech Republic (Program COST, No. OC 523.60) and by GACR (grant no. 203/00/1288).

References

[1] G.D. Soraru, Q. Liu, L.V. Interrante, T. Apple, Chem. Mater. 10 (1998) 4047.

[2] D.V. Tsu, G. Lucovsky, B.N. Davidson, Phys. Rev. B 40 (1989) 1795.

[3] A.M. Wilson, G. Zank, K. Eguchi, W. Xing, B. Yates, J.R. Dahn, Chem. Mater. 9 (1997) 1601.

[4] S. Dire, R. Campostrini, R. Ceccato, Chem. Mater. 10 (1998) 268.

[5] Y.E. Kortobi, J.B. Esoinose la Caillerie, A.P. Legrand, X. Armand, N. Herlin, M. Cauchetier, Chem. Mater. 9 (1997) 632.

[6] T. Fujii, T. Yokoi, M. Hiramatsu, M. Nawata, M. Hori, T. Goto, S. Hattori, J. Vac. Sci. Technol. B 15 (1997) 746.

[7] J. Pola, M. Urbanová, Z. Bastl, J. Šubrt, P. Papagiannakopoulos, J. Mater. Chem. 10 (2001) 1415.

[8] P. John, I.M. Odeh, M.J.K. Thomas, M.J. Tricker, J.I.B. Wilson, Phys. Status Solidi B 105 (1981) 499.

[9] J. Pola, M. Urbanová, Z. Bastl, J. Šubrt, H. Beckers, J. Mater. Chem. 9 (1999) 2429.

[10] J. Pola, Z. Bastl, M. Urbanová, J. Šubrt, H. Beckers, Appl. Organomet. Chem. 14 (2000) 453.

[11] G. Raabe, J. Michl, in: S. Patai, Z. Rappoport (Eds.), The Chemistry of Organic Silicon Compounds, Wiley, Chichester, 1989 chapter 17.

[12] S. Nagase, T. Kudo, T. Akasaka, W. Ando, Chem. Phys. Lett. 163 (1989) 23.

[13] T. Akasaka, S. Nagase, A. Yabe, W. Ando, J. Am. Chem. Soc. 110 (1988) 6270.

[14] A. Patyk, W. Sander, J. Gauss, D. Cremer, Angew. Chem. 101 (1989) 920.

[15] M. Trommer, W. Sander, A. Patyk, J. Am. Chem. Soc. 115 (1993) 11775.

[16] H. Bornemann, W. Sander, J. Am. Chem. Soc. 122 (2000) 6727.

[17] I.M.T. Davidson, C.E. Dean, F.T. Lawrence, J. Chem. Soc. Chem. Commun. (1981) 52.

[18] J. Pola, Z. Bastl, J. Šubrt, R. Taylor, J. Mater. Chem. 5 (1995) 1345.

[19] D. Čukanova, J. Pola, J. Organomet. Chem. 453 (1993) 17.

[20] J. Pola, Rad. Phys. Chem. 49 (1997) 151.

[21] J. Pola, Surface Coat. Technol. 100–101 (1998) 408.

[22] Z. Bastl, H. Bürger, R. Fajgar, D. Pokorná, J. Pola, M. Senzlober, J. Šubrt, M. Urbanová, Appl. Organomet. Chem. 10 (1996) 83.

[23] J.H. Scofield, J. Electron. Spectrosc. Relat. Phenom. 8 (1976) 129.

[24] M.P. Seah, in: D. Briggs, M.P. Seah (Eds.), Practical Surface Analysis. Auger and X-ray Photoelectron Spectroscopy, vol. 1, Wiley, Chichester, 1994, p. 201.

[25] R.M. Irwin, J.M. Cooke, J. Laane, J. Am. Chem. Soc. 99 (1977) 3273.

[26] R. Fajgar, J. Vítek, Z. Haas, J. Pola, J. Chem. Soc. Perkin Trans. 2 (1999) 239.

[27] N. Auner, I.M.T. Davidson, S. Ijadi-Maghsoodi, F.T. Lawrence, Organometallics 5 (1986) 431.

[28] C.D. Wagner, in: D. Briggs, M.P. Seah (Eds.), Practical Surface Analysis. Auger and X-ray Photoelectron Spectroscopy, vol. 1, Wiley, Chichester, 1994, p. 595.

[29] F.L. Galeener, G. Lucovsky, Phys. Rev. Lett. 37 (1976) 1414.

[30] G. Lucovsky, C.K. Wong, W.B. Pollard, J. Non-Cryst. Solid 59/60 (1983) 839.

[31] G. Lucovsky, R.J. Nemanich, J.C. Knights, Phys. Rev. B 18 (1978) 4228.

[32] W.B. Pollard, G. Lucovsky, Phys. Rev. B 26 (1982) 3172.

[33] Infrared Structural Correlation Tables and Data Cards, Heyden and Son Ltd., Spectrum House, London, 1969.

[34] G. Lucovsky, J. Yang, S.S. Chao, J.E. Tyler, W. Czubatyj, Phys. Rev. B 28 (1983) 3225.

[35] D.V. Tsu, G. Lucovsky, B.N. Davidson, Phys. Rev. B 40 (1989) 1795.

[36] P. John, I.M. Odeh, M.J.K. Thomas, M.J. Tricker, J.I.B. Wilson, Phys. Status Solidi B 105 (1981) 499.

[37] C. Fischer, H. Kriegsmann, Zeit. Anorg. Allgem. Chem. 367 (1969) 219.

[38] H. Shanks, C.J. Fang, L. Ley, M. Cardona, F.J. Demond, S. Kalitzer, Phys. Status Solidi B 100 (1980) 43.

[39] T. Kudo, S. Nagase, J. Am. Chem. Soc. 107 (1985) 2589.

[40] C.L. Darling, H.B. Schlegel, J. Phys. Chem. 97 (1993) 8207.

[41] B. Ma, N. Allinger, H.F. Schaefer, J. Chem. Phys. 105 (1996) 5731.

[42] B. Ma, H.F. Schaefer, J. Chem. Phys. 101 (1994) 2734.

[43] J.M. Jasinski, R. Becerra, R. Walsh, Chem. Rev. 95 (1995) 1203.

[44] I. Safarik, V. Sandhu, E.M. Lown, O.P. Strausz, T.N. Bell, Res. Chem. Intermed. 14 (1990) 105.

[45] J. Pola, J. Ludvík, J. Chem. Soc. Perkin Trans. II (1987) 1727.